

## Independent Source Separation of MEG Data and its Evaluation

Yoshio Konno<sup>1</sup>, Jianting Cao<sup>2,3</sup>, Takayuki Arai<sup>1</sup>, Tsunehiro Takeda<sup>4</sup> and Hiroshi Endo<sup>5</sup>.

<sup>1</sup> Department of Electrical and Electronics Engineering, Sophia University,  
7-1 Kioicho, Chiyoda-ku, Tokyo 102-8554, Japan.

<sup>2</sup> Department of Electronics Engineering, Saitama Institute of Technology,  
1690 Fusaiji, Okabe, Saitama 369-0293, Japan.

<sup>3</sup>Brain Signal Processing, RIKEN,  
2-1 Hirosawa, Wako-shi, Saitama 351-0198, Japan.

<sup>4</sup> Department of Complexity of Science and Engineering, Graduate School of Tokyo University,  
7-3-1 Hongo, Bunkyo-ku, Tokyo 113-8656, Japan.

<sup>5</sup> National Institute of Bioscience and Human-Technology,  
1-1-1 Tsukuba-shi-higashi, Ibaraki 305-8566, Japan.

Phone: +81-3-3238-3411, Fax: +81-3-3238-3321, E-mail : yo-konno@sophia.ac.jp

### 1. Introduction

Independent component analysis (ICA) has been applied to electroencephalographic (EEG) or magnetoencephalographic (MEG) data to determine the behavior and localization of brain sources [1, 2, 3, 4, 5, 6]. When detecting an MEG signal, spontaneous and environmental noises may seriously effect recorded data because the magnetic field of brain signals is weak, particularly in the case of non-averaged single-trial data. The most widely used technique for reducing instrumental and environmental noises is to take an average across many stimulation trials. In fact, when applying ICA to MEG data, most researchers have treated averaged data. However, by taking an average, important information is lost, making it advantageous to decrease the number of averages across data trials. The disadvantage of having fewer averages is that because SNR is very poor, the decomposition of a low-power source signal from recorded data is still influenced by noise.

In this paper, we deal with non-averaged single-trial data and averaged multiple-trials data, in order to study the relationship between the accuracy of decomposed brain sources and the number of averages across data trials. To evaluate the results of the performance of decomposition, we focus on: 1) the power of decomposed components and 2) the accuracy of source estimation.

When applying ICA to physiological data, most researchers have used real, measured, physiological data and evaluated the decomposed components for neuroscience perspective. In this study, we use a synthesized MEG data set, which includes an artificial evoked field and real, measured brain data. The behavior of our data set is similar to auditory evoked fields (AEFs). The main advantage of our data set is that dipole location of evoked responses and its dynamics are known in advance, which facilitates the evaluation of the

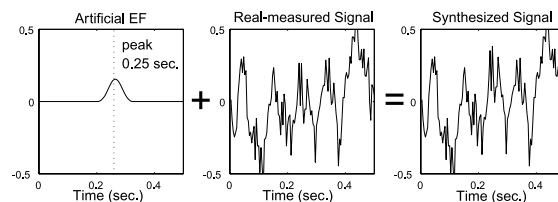


Figure 1: An example for data synthesizing: (left) artificial EF signals, (middle) real measured MEG signals, (right) synthesized signals.

decomposed components.

### 2. Data Analysis Method

#### 2.1. Data Analysis Model

In this section, we describe the model for applying ICA to MEG data. Based on the principle of MEG measurement, this problem can be formulated as

$$\mathbf{x}(t) = \mathbf{A}s(t) + \mathbf{e}(t), \quad (1)$$

where  $\mathbf{x}(t)$ ,  $\mathbf{s}(t)$  and  $\mathbf{e}(t)$  represent the transpose of  $m$  observations at time  $t$ ,  $n$  unknown source components and additive noise, respectively. Since neither human tissue nor skull attenuate magnetic fields in MEG,  $\mathbf{A}$  can be represented by a numerical matrix whose element  $a_{ij}$  is simply a quantity related to the physical distance between the  $i$ -th sensor and the  $j$ -th source.

In the model,  $\mathbf{s}(t)$ ,  $\mathbf{e}(t)$ ,  $\mathbf{A}$  and  $n$  are unknown but  $\mathbf{x}(t)$  are accessible. It is assumed that the components of  $\mathbf{s}(t)$  are mutually statistically independent, as well as statistically independent of the noise components ( $\mathbf{e}(t)$ ). Moreover, the noise components themselves are assumed to be mutually independent.

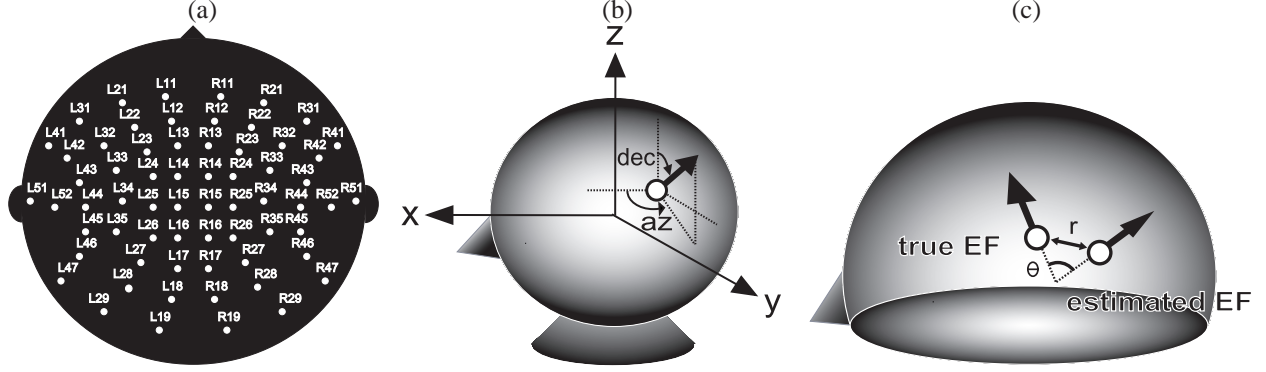


Figure 2: (a) Sensor distribution. (b) 3D frames of reference. (c) Distance  $r$  between true and estimated dipole location and angle  $\Theta$  between true and estimated direction vector.

Table 1: Artificial evoked fields.

peak time (sec.)	location $x, y, z$ (mm)	vector $az, dec$ (deg.)	moment $Q$ (nAm)
0.25	10.0, 10.0, 60.0	50.0, 103.0	40.0

## 2.2. Pre-whitening

In this subsection, we describe our robust pre-whitening technique [2, 3]. This technique is very effective in reducing the power of sensor noises. Applying our robust pre-whitening technique, a new data vector can be obtained by

$$\mathbf{z}(t) = \mathbf{Q}\mathbf{x}(t). \quad (2)$$

where the power of noises, mutual correlation and dimensionality have been reduced. Here,  $\mathbf{Q} \in \mathbf{R}^{n \times m}$  is termed the transform matrix which can be obtained as  $\mathbf{Q} = [\hat{\mathbf{A}}^T \hat{\Psi}^{-1} \hat{\mathbf{A}}]^{-1} \hat{\mathbf{A}}^T \hat{\Psi}^{-1}$ . For this technique,  $\mathbf{A}$  and  $\Psi$  can be estimated as  $\hat{\mathbf{A}} = \mathbf{U}_{\hat{n}} \Lambda_{\hat{n}}^{\frac{1}{2}}$  and  $\hat{\Psi} = \text{diag}(\mathbf{X}\mathbf{X}^T - \hat{\mathbf{A}}\hat{\mathbf{A}}^T)$  by applying the standard PCA approach and the eigenvalue decomposition method, respectively. Here  $\mathbf{X}$  denotes a data matrix of  $\mathbf{x}$ ,  $\Lambda_{\hat{n}}$  is a diagonal matrix whose elements are eigenvalues of  $\mathbf{X}\mathbf{X}^T$ , the columns of  $\mathbf{U}_{\hat{n}}$  are the corresponding eigenvectors and  $\hat{n}$  is the estimated number of sources.

A similar noise reduction approach that applies factor analysis (FA) to the decomposition of MEG data has been reported in [4]. Both this method and ours take additive noises into account, but with our robust pre-whitening technique, the distribution of additive noises is not restricted. Therefore, our technique is more robust and effective for data with non-Gaussian noises such as the outlier.

## 2.3. ICA algorithm

After pre-processing the data, the decomposed independent sources  $\mathbf{y} \in \mathbf{R}^n$  can be obtained from a linear transformation as

$$\mathbf{y}(t) = \mathbf{W}\mathbf{z}(t) = \mathbf{W}\mathbf{Q}\mathbf{x}(t), \quad (3)$$

where  $\mathbf{W} \in \mathbf{R}^{n \times n}$  is termed the demixing matrix which can be computed by using the JADE algorithm [5].

The JADE algorithm has two procedures termed ‘‘orthogonalization in PCA’’ and ‘‘rotation’’. We applied the rotation procedure in the JADE algorithm and calculate the correct rotation matrix  $\mathbf{W}$ . But instead of the orthogonalization in PCA, we applied our robust pre-whitening technique.

To compare the power of decomposed components, we forced every element to be zero except the  $k$ -th ( $k = 1, \dots, \hat{n}$ ) of  $\mathbf{y}(t)$  and obtained the virtual sensor signals coming from  $k$ -th individual components as  $\hat{\mathbf{x}}_k(t) = \hat{\mathbf{A}}\mathbf{W}^{-1}[0 \dots \mathbf{y}_k(t) \dots 0]^T$ . Using the above result, the total sum of each virtual sensor signal coming from the  $k$ -th individual component can be obtained by  $\mathbf{v}_k(t) = \frac{1}{M} \sum_{i=1}^M \hat{\mathbf{x}}_{k,i}(t)$ , where  $M$  denotes the number of sensors and  $\hat{\mathbf{x}}_{k,i}$  denotes the  $k$ -th decomposed components of  $\mathbf{y}(t)$  into the  $i$ -th sensor.

In this study, we define the power of the  $k$ -th decomposed components  $\mathbf{v}_k$  as  $P_{v_k} = \sum_{t=1}^N \mathbf{v}_k(t)\mathbf{v}_k^T(t)$ , where,  $N$  denotes the number of data samples. Applying  $P_{v_k}$  as the power of the  $k$ -th decomposed components, we can compare the power of individual components decomposed by ICA.

## 3. MEG data Analysis

### 3.1. MEG data set

In this subsection, we describe the synthesized MEG data set, which is similar to AEFs, used for simulation. We synthesized an artificial signal and a real measured MEG signal which was recorded by using an Omega-64 (CTF Systems Inc., Canada) (see Fig. 1). The sensor arrays consisted of 64 channels (see Fig. 2(a)). The sampling rate was 250 Hz with a duration of 50 sec.. The observed data was segmented into 100 trials, so the duration of each trial is 0.5 sec. and each trial has 125 samples, where  $i$  denotes the trial number.

The source signals in this data set include evoked field response as well as the 50 Hz electrical power interference and the  $\alpha$ -wave component involved in the real measured MEG data. The evoked field signal was artificially evoked from 0.2 sec. to 0.3 sec. with a peak at 0.25 sec. (see Fig. 1). The

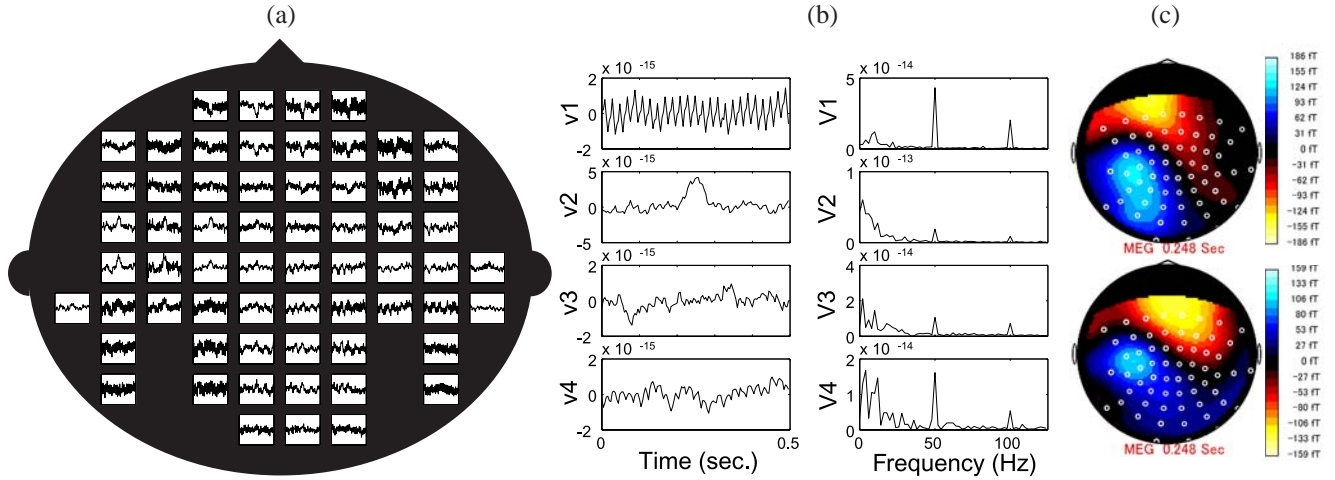


Figure 3: (a) Averaged of 50 trials from 1 to 50 trial. (b) Result of source decomposition and its frequency contents. (c) Estimated map focusing on evoked field,

location  $[x, y, z]$  (mm), direction vector [azimuth:  $az$ , declination:  $dec$ ] (deg.), and dipole moment  $Q$  (nAm) are set as shown in Tab. 1, where a head model presupposes a sphere with a radius of 75 mm and 3D frames of reference are set according to Fig. 2(b).

### 3.2. Simulation Method

In this subsection, we explain the simulation method and evaluation method. To study the relationship between the accuracy of decomposed brain sources and the number of averages across data trials, we take averages across different numbers of trials from 1 to 100-trials. In each averaging process, we use 30 moving samples.

In this study, we focused on the decomposed evoked field signal,  $\alpha$ -wave component and electrical power interference. To classify the decomposed components into these 3 components, we apply an automatic classifying approach [2].

To study the relationship between the power of decomposed components and the number of averages, we take an average of the power of decomposed evoked field signal,  $\alpha$ -wave component and electrical power interference. To study the relationship between the estimation error of evoked field and the number of averages, we apply dipole estimation focusing on evoked response to observed signal and the decomposed evoked signal. We used the standard spatio-temporal dipole fitting routine, MEG v3.3a (CTF System Inc., Canada), to locate the dipole. In this study, since dipole locations and direction vector of evoked field were known in advance, we can compare them to the estimated ones. Here we define the distance  $r$  between true and estimated dipole location and the angle  $\Theta$  between true and estimated direction vector as

$$r = \sqrt{(x - \hat{x})^2 + (y - \hat{y})^2 + (z - \hat{z})^2}, \quad (4)$$

$$\Theta = \cos^{-1}[\sin(d)\sin(\hat{d})\cos(a - \hat{a}) + \cos(d)\cos(\hat{d})] \quad (5)$$

respectively, where  $a$  denotes azimuth (deg.) and  $d$  denotes declination (deg.) (see Fig. 2(c)).

### 3.3. Simulation Results

In this subsection, we first demonstrate the results of the source decomposition and localization for the averaged 50-trials data, as shown in Fig. 3(a). In this figure, the horizontal axis and vertical axis express time from 0 to 0.5 sec. and amplitude from -0.5 to 0.5 pT. In this simulation, the number of sources is assumed to be  $\hat{n} = 4$ . The results  $\mathbf{v}(t)$  and the power spectrums  $\mathbf{V}_k(f)$  are shown in Fig. 3(b).

Applying automatic classifying approach to these decomposed components,  $\mathbf{v}_1$  and  $\mathbf{v}_2$  in Fig. 3(b) are regarded as electrical power interference and evoked field response, respectively. The estimated maps derived by averaged observation and decomposed evoked response are shown in Fig. 3(c). In these figures, the amplitude information appears in the color scale bar. As for the result of evoked response, note that the evoked response appears on the left-front area of the brain. The estimated dipole information of evoked field is shown in Tab. 2. Comparing the results of the ICA and taking averages (before ICA), we conclude that both source location and direction vector become more accurate by applying our ICA approach.

Next, we demonstrate the relationship between the power of each decomposed component and the number of averages. The results are shown in Fig. 4. As for the power of electrical power interference and  $\alpha$ -wave component, the larger the number of averages, the lower the power of these components become. This means that these components are influenced by taking an average. In contrast, the power of evoked response is not influenced by taking average. This means that our ICA approach is very efficient for source decomposition and estimation. But as for single-trial data analysis, the power of evoked field becomes very large, because of the influence of

Table 2: estimated map and estimation error

	dipole location (mm)				direction vector (deg.)		
	$x$	$y$	$z$	$r$	$az$	$dec$	$\Theta$
true value	10.0	10.0	60.0	-	50.0	103.0	-
before ICA	6.1	25.3	64.9	16.5	54.5	111.5	9.6
after ICA	9.8	11.6	71.5	11.6	56.3	101.9	6.3

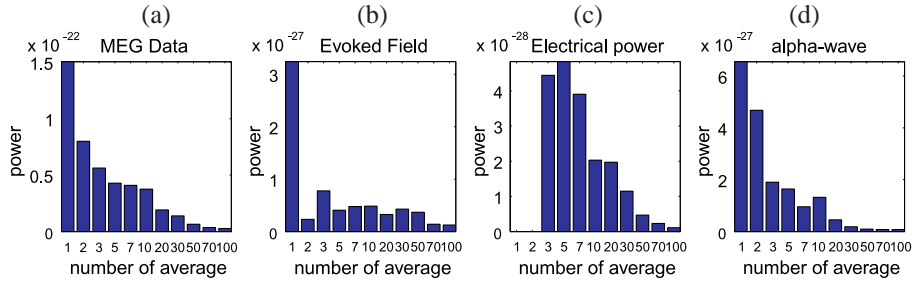


Figure 4: power of decomposed components : (a) averaged observation (b) decomposed evoked response (c) decomposed electrical interference (d) decomposed  $\alpha$ -wave component

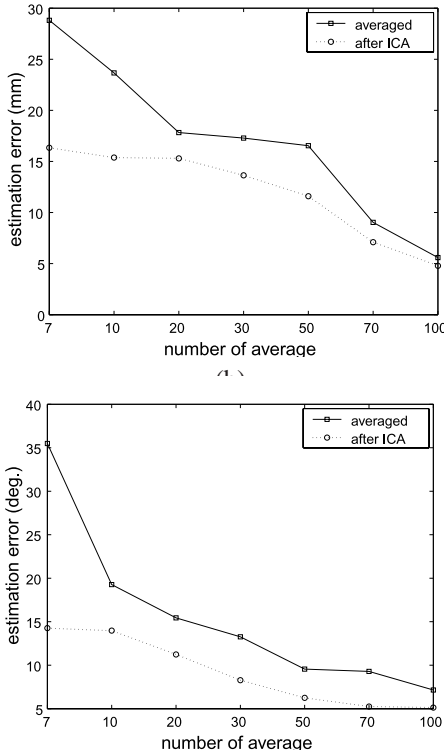


Figure 5: estimation error: (a) dipole location (b) direction vector

additive noise.

Finally, we demonstrate the relationship between the estimation error of each decomposed component and the number of averages. The results are shown in Fig. 5. These results show that, by applying our ICA algorithm, we can reduce the number of average across data trials. Moreover our ICA approach is more effective for the analysis of data with fewer averages than with more averages.

#### 4. Conclusions

In this paper, we performed source decomposition of averaged multiple-trials MEG data using our ICA approach. Our results showed the relationship between the accuracy of source decomposition and the number of averages across data trials.

#### References

- [1] Y. Konno, J. Cao and T. Takeda , “Decomposition and Localization of MEG Brain Sources,” *Journal of Signal Processing*, Vol. 6, No. 6, pp. 391-400, Nov 2002.
- [2] Y. Konno, J. Cao, T. Arai and T. Takeda, “Visualization of Brain Activities of Single-Trial and Averaged Multiple-Trials MEG Data,” *IEICE Trans. on Fundamentals*, Vol. E86-A, No. 9, pp. 2294-2302, Sep 2003.
- [3] J. Cao, N. Murata, S. Amari, A. Cichocki and T. Takeda, “A robust approach to independent component analysis of signals with high-level noise measurements,” *IEEE Trans. on Neural Networks*, Vol. 14, No. 3, pp. 631-645, June 2003.
- [4] S. Ikeda, K. Toyama, “Independent component analysis for noisy data - MEG data analysis,” *Neural Networks* 13, pp. 1063-1074, 2000.
- [5] J. F. Cardoso and A. Souloumiac, “Jacobi angles for simultaneous diagonalization,” *SIAM J. Mat. Anal. Appl.*, Vol. 17, No. 1, pp. 145-151, 1996. Matlab code in WWW : <http://sig.enst.fr/cardoso/jointdiag.html>
- [6] Vigario, R., Sarela, J., Jousmiki, V., Hamalainen, M. and Oja, E, “Independent component approach to the analysis of EEG and MEG recordings,” *Biomedical Engineering, IEEE Transactions on*, Vol. 47 Issue. 5, pp. 589-593, May 2000